J Mater Sci (2010) 45:3448–3456
DOI 10.1007/s10853-010-4372-0

As-cast microstructure and solidification behavior of a high Al- and Nb-containing superalloy

Lianxu Yu · Yating Zhao · Shulin Yang · Wenru Sun · Shouren Guo · Xiaofeng Sun · Zhuangqi Hu

Received: 23 July 2009 / Accepted: 1 March 2010 / Published online: 23 March 2010

Abstract This study investigated the as-cast microstructure and solidification behavior of a high Al- and Nb-containing low thermal expansion IN783 alloy. By analyzing the as-cast microstructure, the quenched microstructure after soaking at high temperature and differential scanning calorimeter (DSC) results, the solidification sequence of IN783 alloy was determined as follows: $L \rightarrow L + \gamma \rightarrow L + \gamma + \beta \rightarrow \gamma + \beta +$ Laves. Segregation of Al and Nb promoted the formation of Al-enriched β phase and Nb-enriched Laves phase, respectively. Several types of β and Laves phase were observed, which were believed to form by different mechanisms and at different stages during solidification.

Introduction

Low coefficient of thermal expansion (CTE) superalloys are used in selected gas turbine components due to their tighter clearance control, which enhances engine efficiency. IN783 alloy (nominal composition of Ni–34Co–26Fe–5.4Al–3Nb–3Cr) is a newly developed low CTE superalloy with superior properties, characterized with a high Al content and a γ–γ'–β three phase microstructure [1–10]. In IN783 alloy, the mechanical properties, especially the fatigue crack propagation rate, are significantly affected by intergranular β phase [2–5]. Therefore, controlling the precipitation of β phase is critical to the performance of IN783 alloy.

Recent studies on controlling β phase are mainly through controlling the hot working and heat treatment processes [3–7]. The high Al β phase formed during solidification process in EXP. 4005 alloy is found to be very difficult to be homogenized, and the remained β phase complicates the microstructure control in the subsequent hot working and heat treatment processes [2]. However, in IN783 alloy, studies on β phase forming during solidification are few. Han et al. [8] reported the segregation characteristics of Nb and Al in IN783 alloy, but they did not address interdendritic segregation of Al and its effect on the solidification behavior. Furthermore, compared with conventional Nb-containing superalloys like IN718 and IN909 [11, 12], Al is also much higher in IN783 alloy which is believed to complicate the solidification process.

The present study investigates the as-cast microstructure, elements segregation, and solidification behavior of the high Al- and Nb-containing IN783 alloy industrial ingot in order to guide the subsequent hot working process to better control the β phase.

Experimental procedure

The Shanghai Baoshan Iron & Steel Corporation provided sample material cutting from casting head of ϕ 423 mm IN783 ingot manufactured by vacuum induction melting (VIM) plus vacuum arc re-melting (VAR). The chemical composition is shown in Table 1. Metallurgical analysis were carried out on the samples cutting from center, 1/2 radius and periphery of the casting head.

L. Yu · S. Yang · W. Sun (✉) · S. Guo · X. Sun · Z. Hu
Institute of Metal Research, Chinese Academy of Sciences, 110016 Shenyang, People's Republic of China
e-mail: wrsun@imr.ac.cn

Y. Zhao
Baoshan Iron & Steel Co., Ltd, Special Steel Branch, 200940 Shanghai, People's Republic of China

Table 1 Chemical composition of the tested IN783 alloy (mass fraction, %)

Cr	Al	Nb	Ni	Fe	Ti	Y	C	Si	Co
2.80	5.40	3.32	28.10	24.88	0.21	0.02	0.02	0.08	Bal.

Differential scanning calorimeter (DSC) examination was performed on a SETSYS Evolution 18 DSC instrument (a product of Setaram Corporation, Caluire, France) in an argon-controlled environment. The temperature measurements were carried out by a (platinum–30% rhodium) versus (platinum–6% rhodium) thermocouple. The temperature calibration was carried out by using the melting point of high-purity Au ($T_m = 1064.4$ °C) and Pd ($T_m = 1{,}551$ °C). The measurement was conducted on a sample cutting from center of the casting head to characterize the solidification sequence. The sample was cut into 3 mm in length and 1 mm in diameter, and the weight was about 144 mg. The high-purity Al_2O_3 cup was employed as the crucible. The heating rate was controlled at 10 °C/min from 1,100 to 1,450 °C.

In order to measure the incipient melting temperature, confirm the solidification sequence, and investigate the influence of cooling rate on precipitation behavior, several samples near center of the ingot were embedded in Al_2O_3 crucible enveloped with Al_2O_3 powders and then heat treated by the processes as listed in Table 2. In order to reveal microstructure, samples before and after heat treatments were electrolytically etched in a solution of 10 vol% phosphoric acid at a voltage of 10 V.

Optical microscopy and scanning electron microscopy (SEM) examinations as well as energy dispersive spectrum (EDS) analysis were carried out to characterize the microstructures of the samples. Element distributions in the samples with heat treatments were analyzed by electron probe micro-analysis (EPMA) examination and the beam size was 1 μm.

Table 2 Heat treatments employed

No.	Detailed heat treatment process
HTS-1	1,160 °C, 0.5 h, (water quench) W.C.
HTS-2	1,170 °C, 0.5 h, W.C.
HTS-3	1,180 °C, 0.5 h, W.C.
HTS-4	1,200 °C, 0.5 h, W.C.
HTS-5	1,220 °C, 0.5 h, W.C.
HTS-6	1,200 °C, 10 °C/min, 1,420 °C, 5 min, 5 °C/min, 1,350 °C, 3 min, W.C.
HTS-7	1,200 °C, 10 °C/min, 1,420 °C, 5 min, 5 °C/min, 1,300 °C, 3 min, W.C.

Results

As-cast microstructure

As-cast microstructures at different areas of the IN783 alloy ingot are shown in Fig. 1. At periphery of the ingot, grain size is relatively small and grain boundaries are outlined by intergranular β precipitates (Fig. 1a). Within the grains, both primary and secondary dendrite microstructures are relatively fine. At 1/2 radius (Fig. 1b), it was not possible to characterize a full grain at that magnification, which indicates the grain is larger. Within the grain, the primary dendrite arm grows much longer, secondary dendrite also develops sufficiently and tertiary dendrite even grows up. When it comes to the center of the ingot (Fig. 1c), the secondary dendrite arm becomes much coarser. The mean values of secondary dendrite arm spacing (SDAS) are listed in Table 3. It can be seen that SDAS increases from periphery to center of the ingot.

The back-scattered electron (BSE-SEM) images in Fig. 2 show the interdendritic precipitates at periphery, 1/2 radius, and center of the ingot. The amount of intergranular precipitates increases significantly from periphery to center of the ingot. At ingot periphery, only a few small white precipitates exist in the interdendritic zone (Fig. 2a). At 1/2 radius, the amount of interdendritic precipitates rises and the precipitate size becomes larger (Fig. 2b). At center, the interdendritic precipitates are markedly increased with the biggest size (Fig. 2c, d). Most of the interdendritic zone is occupied by white precipitates (Fig. 2c), whereas, in some other interdendritic zone, black blocky particles are the most favored precipitates (Fig. 2d).

At center, the interdendritic microstructure is observed at a higher magnification as shown in Fig. 3. The large black blocky precipitates are generally observed to be enveloped by white precipitates (Fig. 3a) or the eutectic mixture (Fig. 3b), which indicates the white phase and black phase are closely related. By analyzing composition characteristics of the precipitates from EDS spectrum, the white precipitates are identified as Nb-enriched Laves phase (Fig. 3c) and the large black blocky precipitate is identified to be Al-enriched β phase (Fig. 3d).

Inside of the large blocky β phase, some much finer white Laves particles are accidentally found as shown in the Fig. 4a, which has never been reported in the casting IN783 alloy before. Figure 4b shows the magnified microstructure of the interdendritic white precipitates widely distributed in the as-cast IN783 alloy which are shown in Fig. 2b, c. Besides the γ and Laves eutectic mixture, many small β particles are also observed at the periphery of the γ and Laves eutectic. At grain boundaries as shown in Fig. 4c, many rod-shaped β precipitates are found accompanying with a few NbC carbide particles. In

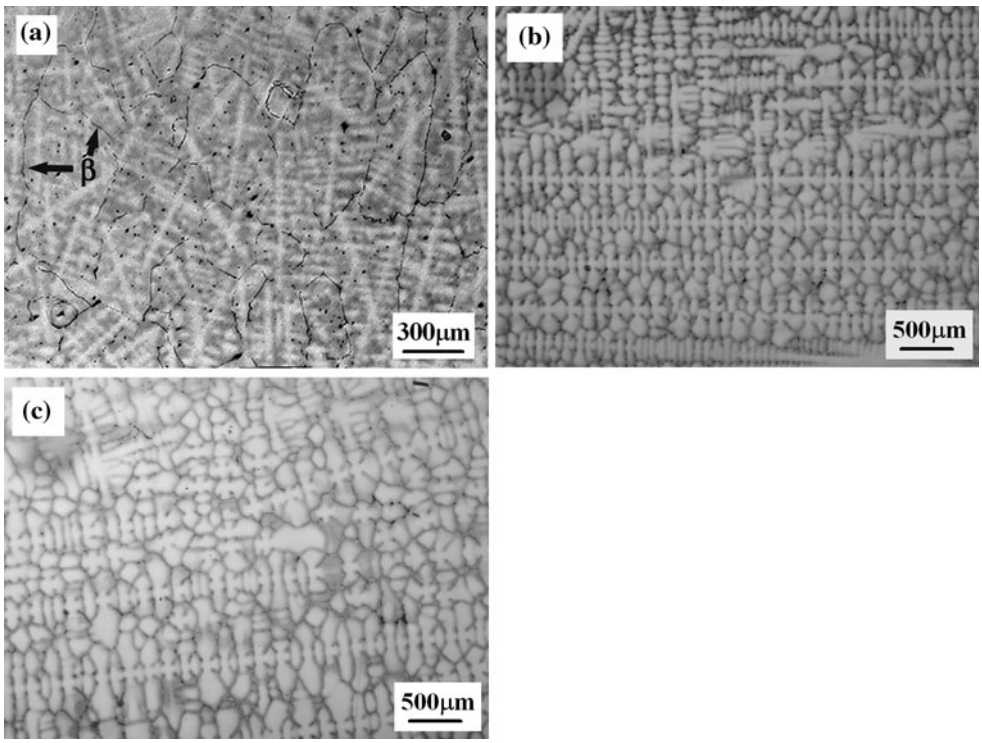

Fig. 1 Optical micrographs showing the dendrite microstructures at the periphery (**a**), 1/2 radius (**b**), and center (**c**) of the as-cast IN783 alloy

Table 3 Secondary dendrite arm spacing (SDAS) at different position of the ingot

Position	Periphery	1/2 radius	Center
SDAS (μm)	50	80	110

sum, it can be concluded that besides Laves phase, two kinds of β phase formed in the as-cast IN783 alloy, which includes the large blocky interdendritic β and the smaller β particles existing at the eutectic periphery and grain boundaries.

Solidification behavior

The as-cast microstructure of IN783 alloy is complex as described above. With the aim of designing homogenization treatment for dissolving the harmful phases which already exist in the original as-cast microstructure, it is essential to further analyze the solidification behavior so that their formation mechanism has to be understood. DSC examination was carried out on the sample cutting from center of the ingot. The DSC curve is shown in Fig. 5. From the full scale curve as shown in Fig. 5a, two endothermal peaks P-H1 and P-H2 are identified from the heating curve and only one exothermal peak P-C1 is identified from the cooling curve. Magnifying the curve ranges from 1,120 to 1,320 °C, another endothermal peak P-H3 is also observed from the on-heating curve, while no endothermal peak can be identified from the on-cooling curve as shown in Fig. 5b. According to reference [13], the start temperature of each reaction is determined to be the onset temperature. The peak and onset temperatures are listed in Table 4. Clearly, there are three major reactions during the heating process: the first reaction (P-H3) starts at about 1,160 °C, the second reaction (P-H2) starts at 1,336 °C, and the third reaction starts at 1,354 °C. However, only one reaction (P-C1) starts at 1,365 °C is identified from the on-cooling curve.

It is reasonable to conclude that the P-H1 peak should be the liquidus temperature of γ phase. In order to characterize the phase transformation reactions corresponding to the other endothermal peaks, samples cutting from the ingot are then soaked, respectively, at 1,160 °C (HTS-1); 1,170 °C (HTS-2); 1,180 °C (HTS-3); 1,200 °C (HTS-4); and 1,220 °C (HTS-5) for 0.5 h and quenched in water afterward. Microstructures of samples with different heat treatments are shown in Fig. 6. In samples soaked at 1,160 and 1,170 °C, the eutectic Laves phase is completely dissolved while only blocky Laves phase is remained around the coarse blocky β phase (Fig. 6a). Elevating the soaking temperature to 1,180 °C, besides the remained NbC and β precipitates, white eutectic is also observed around the β phase (Fig. 6b). As this eutectic microstructure is much finer than the eutectic in the as-cast alloy (Fig. 4b), it is believed to be a Nb-enriched Laves incipient melting pool.

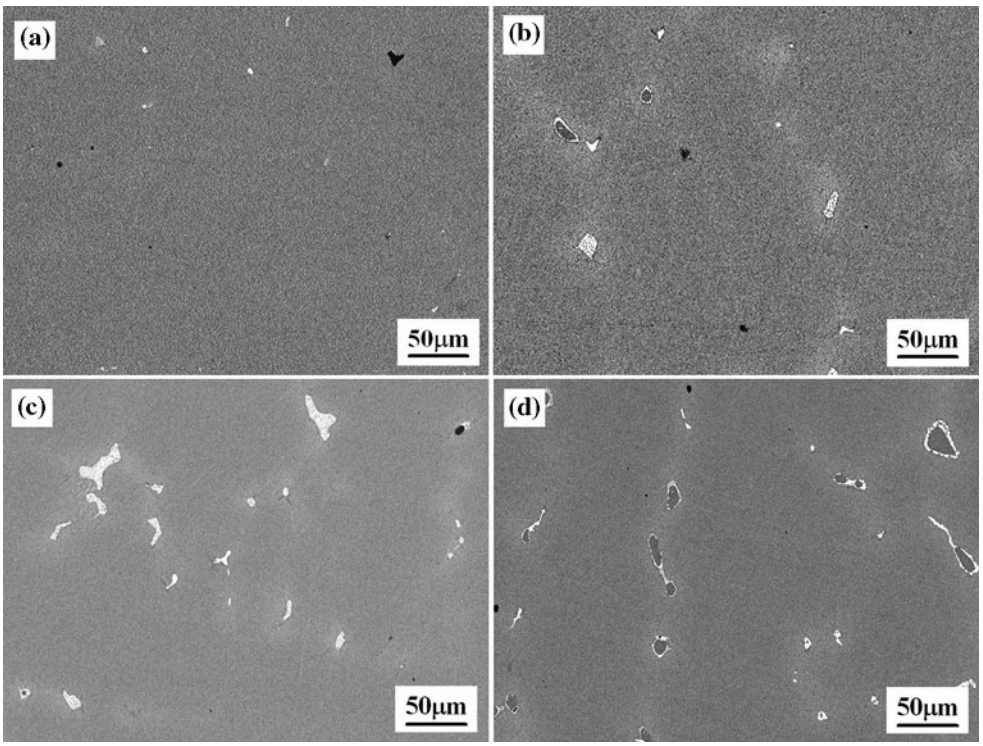

Fig. 2 Back-scattered electron (BSE-SEM) images showing the interdendritic precipitates at the periphery (**a**), 1/2 radius (**b**), center (**c**, **d**) of the as-cast IN783 alloy

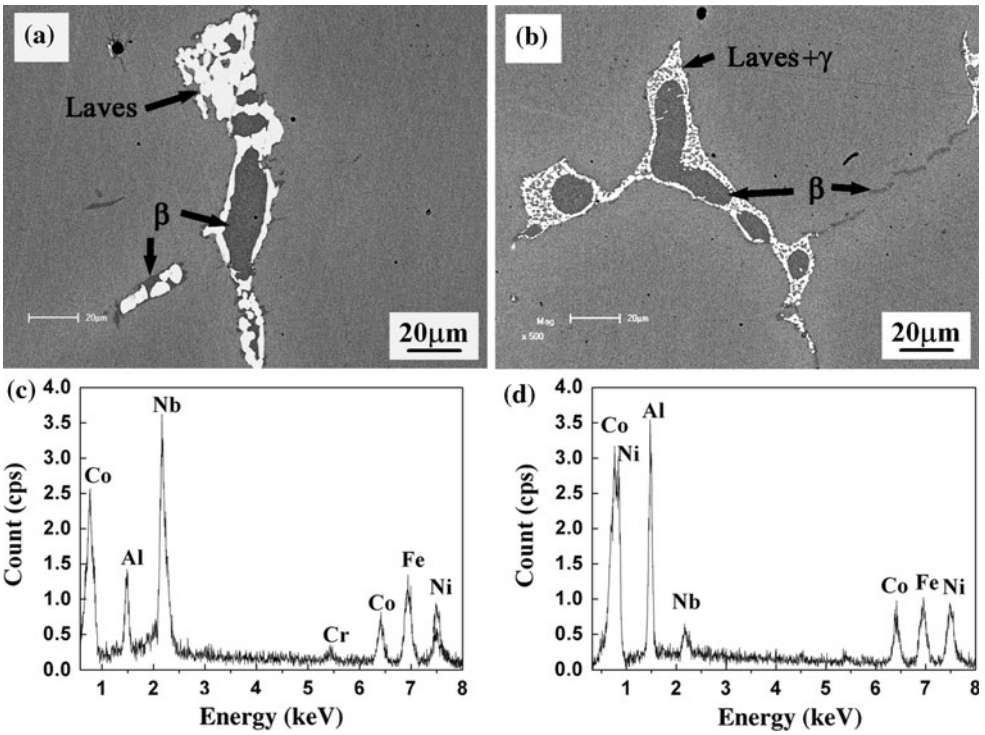

Fig. 3 BSE-SEM images showing the interdendritic precipitates in the as-cast alloy: microstructures (**a**, **b**) and the EDS spectra of the white precipitates (**c**) and the black blocky phase (**d**)

In the sample soaked at 1,200 °C, a much larger incipient melting pool is formed as shown in Fig. 6c. In addition, unlike in the original as-cast microstructure in Fig. 4b, there is no smaller β particle around the fine eutectic (Fig. 6c), which indicates that smaller β particles are not possible to form at fast cooling process. Therefore, they are

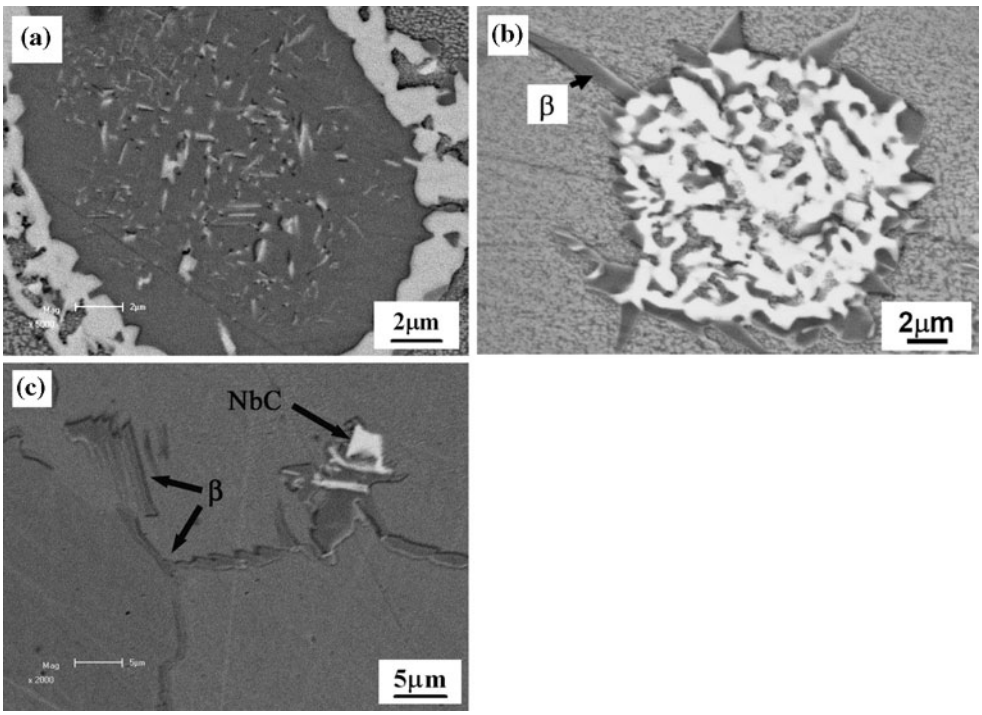

Fig. 4 BSE-SEM images showing the interdendritic precipitates: **a** the large blocky β, **b** the white precipitates in Fig. 2b, c, and **c** intergranular rod-shaped β

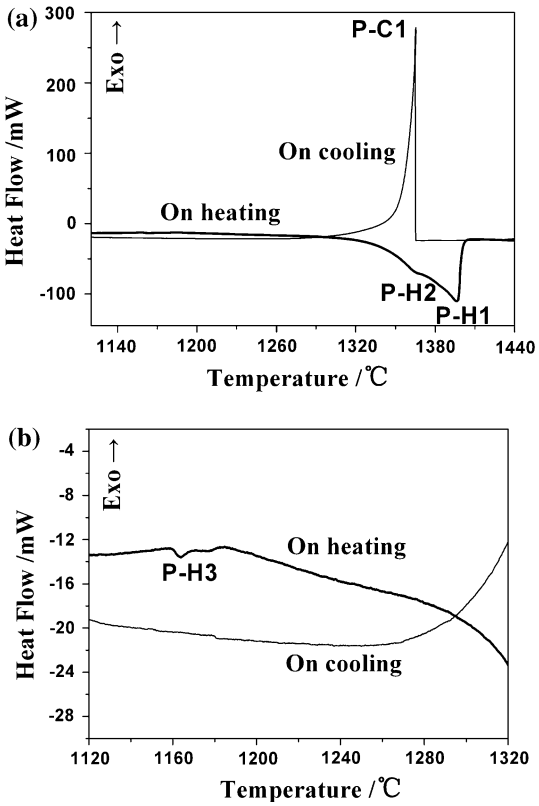

Fig. 5 DSC curves of IN783 alloy **a** full scale and **b** part of the curve

believed to be formed during the cooling process due to diffusion of Al in the solidified alloy. However, in the sample soaked at 1,220 °C, besides the large incipient melting pool, the large blocky β phase still remains as shown in Fig. 6d.

Table 4 Summary of solidification reaction temperatures in the DSC curve in Fig. 5

Peak (°C)	P-H1	P-H2	P-H3	P-C1
Peak temperature	1,396	1,364	1,164	1,365
Onset temperature	1,354	1,336	1,160	1,365

From the above analysis, it can be inferred that the incipient melting phase is Laves phase and the melting temperature is ranged approximately from 1,170 to 1,180 °C. In this alloy, β is a high melting phase because it still exists after soaking at 1,220 °C (Fig. 6d), and its melting reaction is perhaps related with the reaction starting at 1,336 °C in the DSC heating curve.

To identify the phase transformation at 1,349 °C, samples are remelted and then quenched at 1,350 °C (HTS-6) and 1,300 °C (HTS-7) as listed in Table 2. The microstructures are shown in Fig. 7. For the sample treated with HTS-6, the alloy just begins to solidify and a fine dendrite microstructure is produced (Fig. 7a). Thus, relatively fewer solutes are segregated in the interdendritic zone and fine eutectic mixture constituted by β, Laves, and γ is produced (Fig. 7b). Compared Fig. 7b with the quenched microstructure at 1,200 °C (Fig. 6c), these small β particles within the eutectic are the primary solidified β phase which has not able to grown up, and they are believed to be different from these small β particles distributing at the

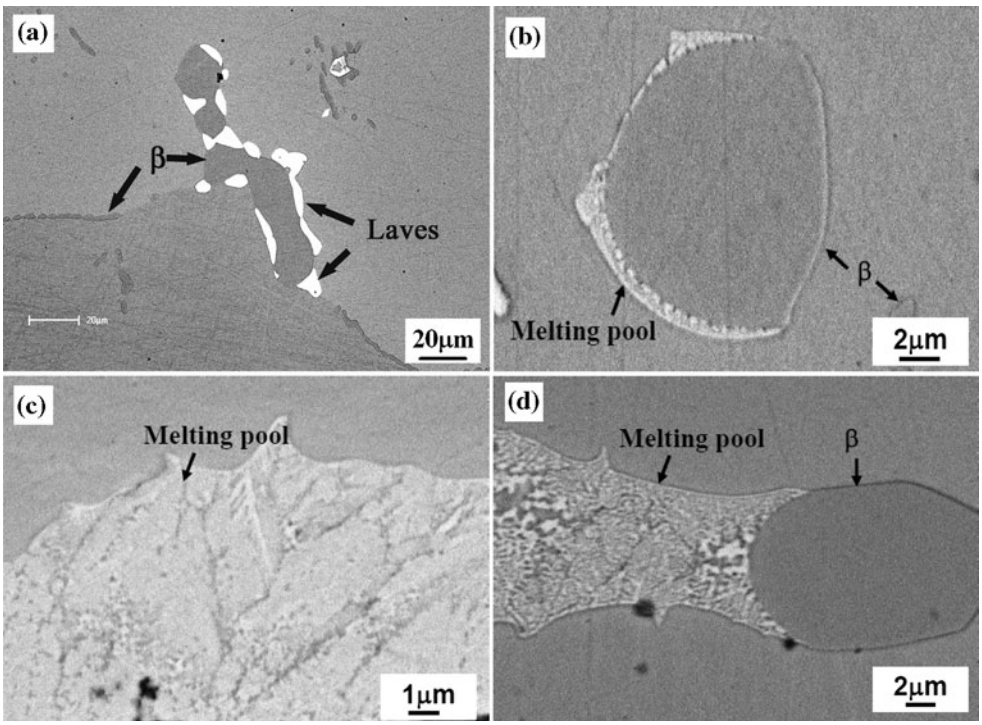

Fig. 6 BSE-SEM images showing microstructures of IN783 alloy quenched at **a** 1,160 °C, **b** 1,180 °C, **c** 1,200 °C, and **d** 1,220 °C

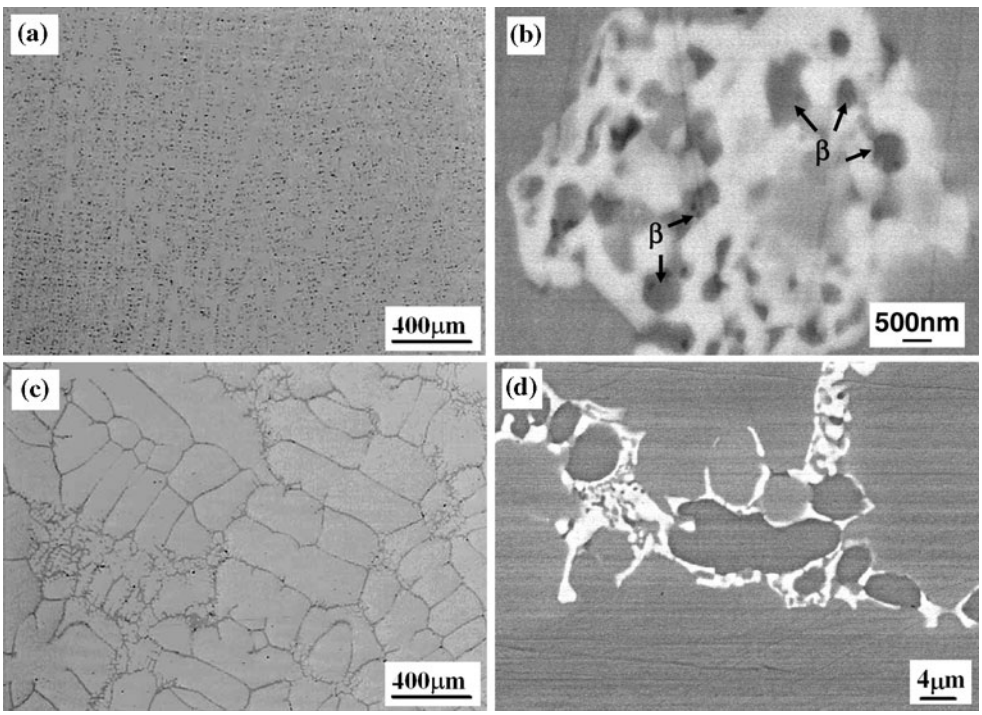

Fig. 7 Dendrite microstructures and interdendritic precipitates in remelted IN783 alloy heat treated by HTS-6 (**a**, **b**) and HTS-7 (**c**, **d**)

periphery of the eutectic (Fig. 4b). In alloy treated with HTS-7, dendrites grow sufficiently, element segregation is enhanced and the residual liquid is able to connect together (Fig. 7c). Due to the enhanced element segregation, the interdendritic precipitates are much larger and coarse blocky β precipitates have already formed (Fig. 7d). The above investigation confirms that there exists a β phase transformation reaction with in the temperature range from 1,300 to 1,350 °C. Therefore, the reaction of P-H2 is believed to be related with the melting of β phase.

Element distribution

In IN783 alloy ingot, Nb-enriched Laves phase and Al-enriched β phase are the major interdendritic phases. To explain the precipitation behavior in IN783 ingot, the element distribution is analyzed by EPMA line scanning analysis of Ni, Al, and Nb in the alloy with HTS-5 and HTS-6. Figure 8 shows the dendritic microstructure of sample after quenching at 1,350 °C. It can be seen that in some interdendritic zone, neither β nor Laves phase is formed, and only element segregation zone is formed which shows a relatively brighter color compared with the dendrite core, but not as bright as the Laves eutectic. Investigation is made along the dark line passing through the dendrite arm, element segregation zone (at the left part of the line), and interdendritic precipitates (at the right part of the line) as marked in Fig. 8a. Both Nb and Al segregate gradually from the dendrite core to the interdendritic zone, which indicates that Al is also a normal segregating element. The segregation of Nb is much severer than Al in both the interdendritic zone with and without precipitates. In some interdendritic zone, accumulation of Nb is high enough to form the white eutectic. Consequently, Al and Ni are depleted there and enriched at the periphery of the white eutectics as shown in Fig. 8b. When cooling to 1,300 °C, the large black blocky β particles have already formed (Fig. 8c). EPMA line scanning analysis is also done across the large black blocky β, as shown in Fig. 8d. It clearly indicates that the solidification of β consumes much Ni and Al, which depletes Ni and Al concentration severely in the residual liquid. And as the solubility of Nb is low in β phase, growth of the large black blocky β rejects Nb into the residual liquid, which consequently promotes the formation of Laves and γ eutectic.

Discussion

From the above experimental results, it is known that the dendrite morphology and grain size vary at different area of the ingot. This is believed to be caused by different local undercooling during solidification. At periphery of the ingot, the undercooling is large and the nucleation rate is high. Therefore, many primary dendrites grow fast and are soon contacted with each other. Hence, the grain is the smallest, and both primary and secondary dendrites are the finest (Fig. 1a). At 1/2 radius and center, the undercooling is lower which decreases the nucleation rate. The heat dissipation capability is also insufficient which makes the freezing rate decrease. Therefore, both primary and secondary dendrites grow sufficiently and the mean dendrite spacing is also enlarged (Fig. 1b, c).

As the solidification rate decreases from the ingot periphery to the ingot center, segregation of alloying elements changes gradually as well which results in different interdendritic microstructure. In the periphery of the ingot, the freezing rate is quite high and the dendritic segregation is not severe, therefore, few interdendritic precipitates can

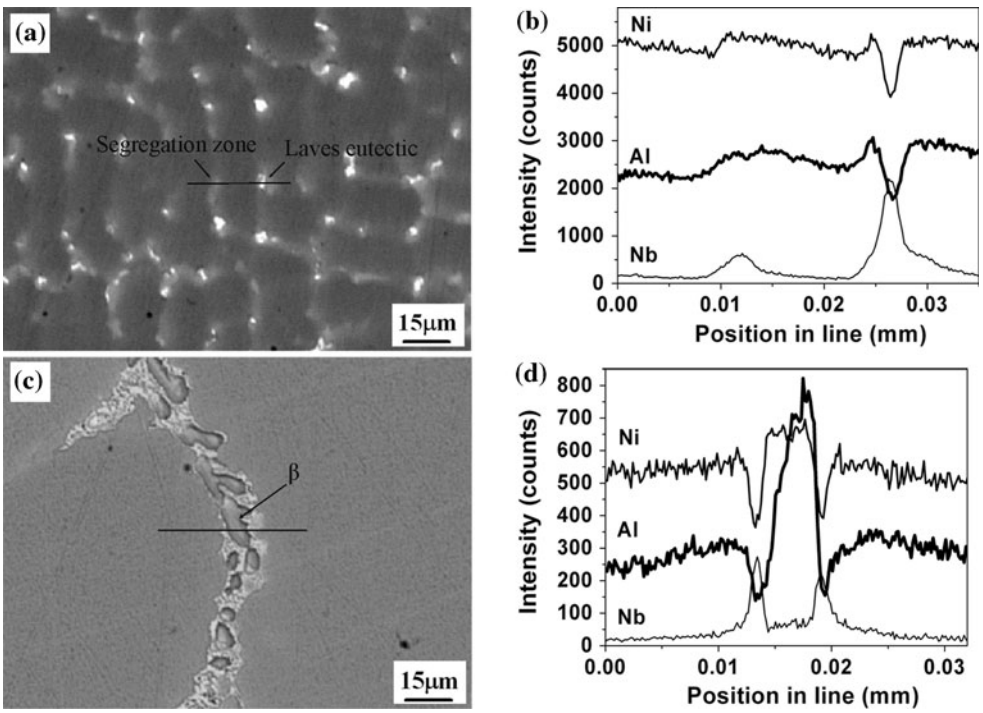

Fig. 8 Microstructures and distribution of Ni, Al, and Nb in remelted IN783 alloy heat treated by HTS-6 (**a**, **b**) and HTS-7 (**c**, **d**)

be formed (Fig. 2a). As the cooling rate decreases from the periphery to center of the ingot, the interdendritic segregation is enhanced, which increases the amount and enlarges the size of interdendritic precipitates (Fig. 2b, c).

The solidification of β phase is also closely related with the cooling rate. During its solidification range, at a fast cooling rate (as water quenched), the element segregation is insufficient, the primary β phase would be much finer and the amount is also limited (Fig. 7b, d). As a result, large β particle is hardly can be found at the periphery of the ingot.

For the DSC sample, the enhanced segregation of Al in the center of the large ingot produces a lot of large β particles, as a result, the melting of these β particles can produce a small endothermal peak starting at 1,336 °C during the heating process. After the sample is fully remelted at 1,396 °C, it has been soaked in liquid condition for nearly 13 min before re-solidifying at 1,365 °C, which is believed to make the solute distribution more homogeneous. Besides the insufficient element segregation, the fast cooling rate (10 °C/min) during DSC experiment is expected to further constrain the formation of large interdendritic precipitates. As a result, there is no other exothermal peak except for the exothermal peak P-C1 at the initial solidification process.

As shown in Fig. 8b, both Nb and Al perform normal segregation and the segregation inclination of Nb is much higher. Such partition behaviors of Nb and Al have also been shown in other superalloys [14–18]. When the ingot is solidified to the β freezing point (ranging from 1,336 to 1,364 °C based on-heating curve in Table 4), in some interdendritic zone with enough Al, large blocky Al-enriched β precipitates are formed. As Nb is not a β former element [19], the formation of large blocky β phase is believed to expel Nb to the residual liquid and promotes the formation of Laves phase (1,170–1,180 °C) (Figs. 3a, b, 8c, d). However, it is impossible to sufficiently expel all the supersaturated Nb atoms out of the large β particle. Therefore, many fine Nb-enriched Laves particles precipitate in the body of the large blocky β phase during cooling as shown in Fig. 4a, and the mechanism is believed to be similar with the case in Ref. [5]. In the solidification of IN783 alloy, the formation of large primary β phase requires much Al, it only forms in some high Al segregating interdendritic zone. Therefore, the formation of large primary β phase is only popular in some of the interdendritic zone.

In most interdendritic zone, the segregation of Nb is predominant which favors the formation of Laves and eutectic. However, due to the limited solubility of Al in Laves phase, Al is excluded to the periphery of the Laves phase which forms many small β particles during the cooling process (Fig. 4b). The formation of these small β particles is in accordance with those at grain boundaries, which is related to the segregation of Al at grain boundaries during cooling from high temperature [8].

Conclusions

The as-cast microstructure and solidification behavior of a high Al- and Nb-containing low thermal expansion IN783 alloy have been studied in detail. Its solidification sequence is determined as follows: $L \rightarrow L + \gamma \rightarrow L + \gamma + \beta \rightarrow \gamma + \beta +$ Laves. Aluminum and niobium promote the precipitation of Al-enriched β phase and Nb-enriched Laves phase, respectively. Two types of β phase are observed: the large blocky particles and the small β particles within the eutectic are the primary phase solidified during the solidification process due to the sufficient segregation of Al, whereas, the small granular particles at periphery of the eutectic or grain boundaries are formed by Al diffusion in the solidified alloy during cooling process. The primary β phase expels Nb greatly in the residual liquid, which promotes the formation of Nb-enriched Laves phase at a lower temperature. Therefore, the large blocky β phase is usually enveloped by Laves precipitates or eutectic ($\gamma +$ Laves). However, in most interdendritic zone, Nb segregation is predominant, and only eutectic ($\gamma +$ Laves) forms finally at about 1,170–1,180 °C.

Acknowledgements This work was financially supported by the National Basic Research Program (973 Program) of China under grant No. 2010CB631200 (2010CB631206), the National Natural Science Foundation of China (NSFC) under grant No. 50931004. The authors are grateful for those supports.

References

1. Smith JS, Heck KA (1996) In: Kissinger RD et al (eds) Superalloys 1996. The Minerals, Metals and Materials Society, Warrendale, p 91
2. Heck KA, Smith DF, Holderby MA, Smith JS (1992) In: Antolovich SD et al (eds) Superalloys 1992. The Minerals, Metals and Materials Society, Warrendale, p 237
3. Ma LZ, Chang K-M, Mannan SK, Patel SJ (2003) Scr Mater 48:551
4. Ma LZ, Chang K-M (2004) J Mater Eng Perform 13:32
5. Han GW, Zhang YY (2006) Mater Sci Eng A 441:253
6. Higginbotham BE, Chang KM, Mannan S, deBarbadillo JJ (1997) In: Proceedings of the first international non-ferrous processing and technology conference, St. Louis, Missouri, p 483
7. Jia XY, Zhao YX, Zhang SW (2006) Mater Eng (in Chinese) Suppl 1:165
8. Han GW, Zhang YY (2005) Mater Sci Eng A 412:198
9. Mannan SK, Smith GD, Patel SJ (2004) In: Green KA et al (eds) Superalloys 2004. The Minerals, Metals and Materials Society, Warrendale, p 627
10. Ott EA, Groh JR, Mannan SK (2004) In: Green KA et al (eds) Superalloys 2004. The Minerals, Metals and Materials Society, Warrendale, p 643

11. Cieslak MJ, Headley TJ, Knorovsky GA, Romig AD Jr, Kollie T (1990) Metall Trans A 21:479
12. Dupont JN, Robino CV, Michael JR, Notis MR, Marder AR (1998) Metall Mater Trans A 29:2785
13. Boettinger WJ, Kattner UR (2002) Metall Mater Trans A 33:1779
14. Schneider MC, Gu JP, Beckermann C, Boettinger WJ, Kattner UR (1997) Metall Mater Trans A 28:1517
15. Ojo OA, Richards NL, Chaturvedi MC (2004) Scr Mater 51:683
16. Zupanič F, Bončina T, Križman A, Tichelaar FD (2001) J Alloys Compd 329:290
17. Sun XF, Yin FS, Li JG, Hou GC, Zheng Q, Guan HR, Hu ZQ (2003) Acta Metall Sin (in Chinese) 39:27
18. Ganesan M, Dye D, Lee PD (2005) Metall Mater Trans A 36:2191
19. Jia CC, Ishida K, Nishizawa T (1994) Metall Mater Trans A 25:473